Frontiers in Bioscience Landmark

Front. Biosci. (Landmark Ed) **2025**; 30(11): 46252
https://doi.org/10.31083/FBL46252

Short Communication

Overexpression of *CSRP1* Suppresses Cell Viability and Enhances the Anti-Cancer Effects of Anti-*PD-L1* Therapy in Renal Cell Carcinoma

Yi He[1], Bo Yang[1], Ying Ke[1], Dianlong Zhang[2], Yiqun Yao[2,*]

[1]Department of Urology, The Second Hospital of Dalian Medical University, 116023 Dalian, Liaoning, China
[2]Department of General Surgery, The Affiliated Zhongshan Hospital of Dalian University, 116001 Dalian, Liaoning, China
*Correspondence: yaoyiqun_rx@163.com (Yiqun Yao)

Academic Editor: Nikos Karamanos
Submitted: 2 September 2025 Revised: 7 October 2025 Accepted: 10 November 2025 Published: 27 November 2025

Abstract

Background: Cysteine and Glycine Rich Protein 1 (*CSRP1*) is a member of the cysteine-rich protein family, characterized by a unique double-zinc finger motif. It plays an important role in development and cellular differentiation. Aberrant expression of *CSRP1* has been reported in several malignancies, including prostate cancer and acute myeloid leukemia. However, its function in renal cell carcinoma (RCC) remains unexplored. In this study, we investigated the role of *CSRP1* in RCC for the first time. **Methods**: *CSRP1* and programmed death-ligand 1 (*PD-L1*) expression levels were determined using quantitative real-time polymerase chain reaction (qRT-PCR). The effects of *CSRP1* overexpression on cellular proliferation, migration, and apoptosis were assessed *in vitro* through CCK-8, wound healing, and flow cytometry assays. To evaluate the role of *CSRP1* in immunotherapy, Balb/c mice were treated with anti-*PD-L1* antibody, and tumor growth was monitored. **Results**: *In vitro*, overexpression of *CSRP1* significantly inhibited proliferation and migration of A498 cells while enhancing their sensitivity to sunitinib treatment. Mechanistically, *CSRP1* overexpression downregulated *PD-L1* expression in RCC cells. In BALB/c mice inoculated with Renca cells, *CSRP1* overexpression led to reduced tumor growth and improved response to anti-*PD-L1* therapy. **Conclusion**: *CSRP1* may play a role in regulating cell viability, migration, drug resistance, and possibly innate immunity in RCC. These findings suggest that *CSRP1* could increase the efficacy of targeted drugs and immunotherapy in combination treatment strategies for RCC.

Keywords: renal cell carcinoma; cysteine and glycine-rich protein 1; cell survival; immunotherapy; Lin-11 Is1-1 Mec-3 domain proteins

1. Introduction

Renal cell carcinoma (RCC) ranks as the second deadliest urological malignancy [1]. Clear cell RCC is the most prevalent histological subtype, comprising approximately 80–90% of all cases. The prognosis for RCC patients remains poor, with 5-year survival rates lingering between 5% and 12% [2]. As such, metastatic RCC management has been dominated by treatment with anti-angiogenic agents, such as the multi-tyrosine kinase inhibitor sunitinib [3]. While 70% of patients experience substantial benefit from sunitinib, a considerable proportion exhibit primary or acquired resistance, leading to eventual disease progression [3]. Thus, there is an urgent need to identify novel therapeutic targets and strategies to improve outcomes for patients with suboptimal response to existing therapies.

The cysteine- and glycine-rich protein (*CSRP*) family belongs to the Lin-11 Is1-1 Mec-3 (LIM) domain superfamily, which is evolutionarily conserved across vertebrates and invertebrates. The LIM domain mediates diverse cellular functions such as gene regulation and cytoskeletal organization [4]. Vertebrates express three *CSRP* members: *CSRP1*, *CSRP2*, and *CSRP3/MLP* [5,6]. Recently, CSRP1 has garnered increasing attention for its potential role in cancer, particularly in urogenital malignancies. It has been implicated in adrenocortical carcinoma [7], prostate cancer [8,9], bladder cancer [10], and kidney papillary cell carcinoma [11]. But most existing evidence relies on bioinformatic predictions, and systematic functional studies are lacking. The specific function of *CSRP1* in RCC remains largely unexplored, representing a critical knowledge gap that warrants further investigation.

Therefore, we aimed to elucidate the functional role of *CSRP1* in RCC through *in vitro* experiments and preclinical mouse tumor models.

2. Materials and Methods

2.1 Cell Culture and Transfections

A498 (#HTB-44) and Renca (#CRL-2947) cell lines were obtained from the American Type Culture Collection (ATCC, Manassas, VA, USA). The cells were maintained in Dulbecco's Modified Eagle Medium (DMEM; #11995065; Invitrogen, Thermo Fisher Scientific, Waltham, MA, USA) supplemented with 10% fetal bovine serum (FBS; #10270106; Invitrogen, Thermo Fisher Scientific, Waltham, MA, USA), 100 U/mL penicillin, and 100 mg/mL streptomycin (Penicillin-Streptomycin Solution; Catalog #: 15140122; Invitrogen, Thermo Fisher Scientific, Waltham, MA, USA). Cultures were incubated at 37 °C in a humidified atmosphere containing 5% CO_2. For *CSRP1* overexpression, 3×10^6 A498 or Renca cells were

Table 1. qPCR primer sequences for RT-PCR.

Human *GAPDH*	Forward: 5′-GCACCGTCAAGGCTGAGAAC-3′ Reverse: 5′-TGGTGAAGACGCCAGTGGA-3′
Human *CSRP1*	Forward: 5′-TGCCGAAGAGGTTCAGTGC-3′ Reverse: 5′-AGCAGGACTTGCAGTAAATCTC-3′
Human *PD-L1*	Forward: 5′-CCTACTGGCATTTGCTGAACGCAT-3′ Reverse: 5′-CAATAGACAATTAGTGCAGCCAGGTC-3′
Mouse *GAPDH*	Forward: 5′-GCACCGTCAAGGCTGAGAAC-3′ Reverse: 5′-TTTGCACTGGTACGTGTTGAT-3′
Mouse *CSRP1*	Forward: 5′-AGCTTCCATAAATCCTGCTTCC-3′ Reverse: 5′-ACTTCTTGCCGTAACATGACTTG-3′
Mouse *PD-L1*	Forward: 5′-TGCTGCATAATCAGCTACGG-3′ Reverse: 5′-GCTGGTCACATTGAGAAGCA-3′

transfected with 2 µg of either pcDNA3.1-*CSRP1* plasmid or empty vector (control) using 6 µL of Lipofectamine 2000 (#11668019; Invitrogen, Thermo Fisher Scientific, Waltham, MA, USA), in accordance with the manufacturer's instructions. Following 48 hours of incubation post-transfection, the cells were reseeded into 10-cm dishes and cultured for an additional 48 hours. Stable cell lines were selected using 1000 µg/mL G418 (#G8168; Sigma-Aldrich, St. Louis, MO, USA) for 20 days. The established lines were named A498-*CSRP1* and Renca-*CSRP1*. All cell lines were validated by STR profiling and tested negative for mycoplasma.

2.2 Quantitative Real-Time PCR (qRT-PCR)

Successful overexpression of *CSRP1* was verified by qRT-PCR. As directed by the manufacturer, RNA was extracted from cells using the RNA isoPlus® Reagent Kit (#9109; Takara, Shiga, Japan). RNA was converted to cDNA using the PrimeScript® RT Reagent Pack (#RR037A; Takara, Shiga, Japan). The SYBR® Premix Ex Taq™ Unit (#RR420A; Takara, Shiga, Japan) was used to amplify the cDNA in accordance with the 7500 Continuous PCR system (Applied Biosystems, Thermo Fisher Scientific, Waltham, MA, USA). The following were the cycling conditions: GAPDH was used as the loading control for the target genes during forty cycles of 95 °C for 30 s and 60 °C for 34 s in the comparative Ct technique of data analysis. The initial sequences were listed in Table 1.

2.3 Flow Cytometry Analysis of Cell Apoptosis

After a 24-hour incubation for attachment, cells seeded in six-well plates (1×10^5 cells/well) were treated with 10 µM sunitinib (#S1042; Selleckchem, Houston, TX, USA). Following treatment, cells were harvested, washed with PBS, and resuspended in 300 µL of binding buffer containing 5 µL of propidium iodide (PI; #P4170; Sigma-Aldrich, St. Louis, MO, USA). After 15 minutes of incubation in the dark, the samples were analyzed on a BD FACSVerse flow cytometer (BD Biosciences, San Jose, CA, USA) to quantify viable, apoptotic, and necrotic populations by PI incorporation.

2.4 Migration Assay

A wound healing assay was performed to evaluate the migratory ability of the cell lines. Cells were seeded in 6-well plates at a density of 1×10^4 cells/mL and cultured at 37 °C under 5% CO_2 until they reached 80% confluence. A uniform scratch was then created in the monolayer using a sterile 20 µL serological pipette tip. After washing with 1 mL of medium to remove detached cells and debris, the cells were incubated in serum-free medium for 12 hours. Cell migration into the wound area was monitored and imaged under a microscope.

2.5 Cell Proliferation Assay

96 well plates were utilized to seed cells (2×10^5 cells/well). The cells were incubated for three hours at 37 °C and 5% CO_2 using the CCK-8 kit from Tiangen (Hangzhou, Zhejiang, China), which was mixed at a volume of 10 µL per well. At long last, we read the absorbance at 450 nm on the microplate peruser (Thermo Fisher Logical, Inc.).

2.6 Animal Study

The animal experiments in this study were conducted in strict compliance with the ARRIVE guidelines, the UK. Animals (Scientific Procedures) Act 1986 and its associated guidelines, and the EU Directive 2010/63/EU. All procedures were reviewed and approved by the Animal Ethics Committee of Dalian Medical University (Permit Number: AEE24139). Male BALB/c nude mice (4–6 weeks old, weighing 20 ± 2 g, n = 10) were housed under specific pathogen-free conditions in individually ventilated cages. The environment was maintained with controlled temperature and humidity and a 12-hour light/dark cycle. Food and water were provided ad libitum. Health status was monitored daily throughout the study. Renca-pcDNA3.1 or Renca-*CSRP1* cells (2×10^6 in 0.1 mL PBS)

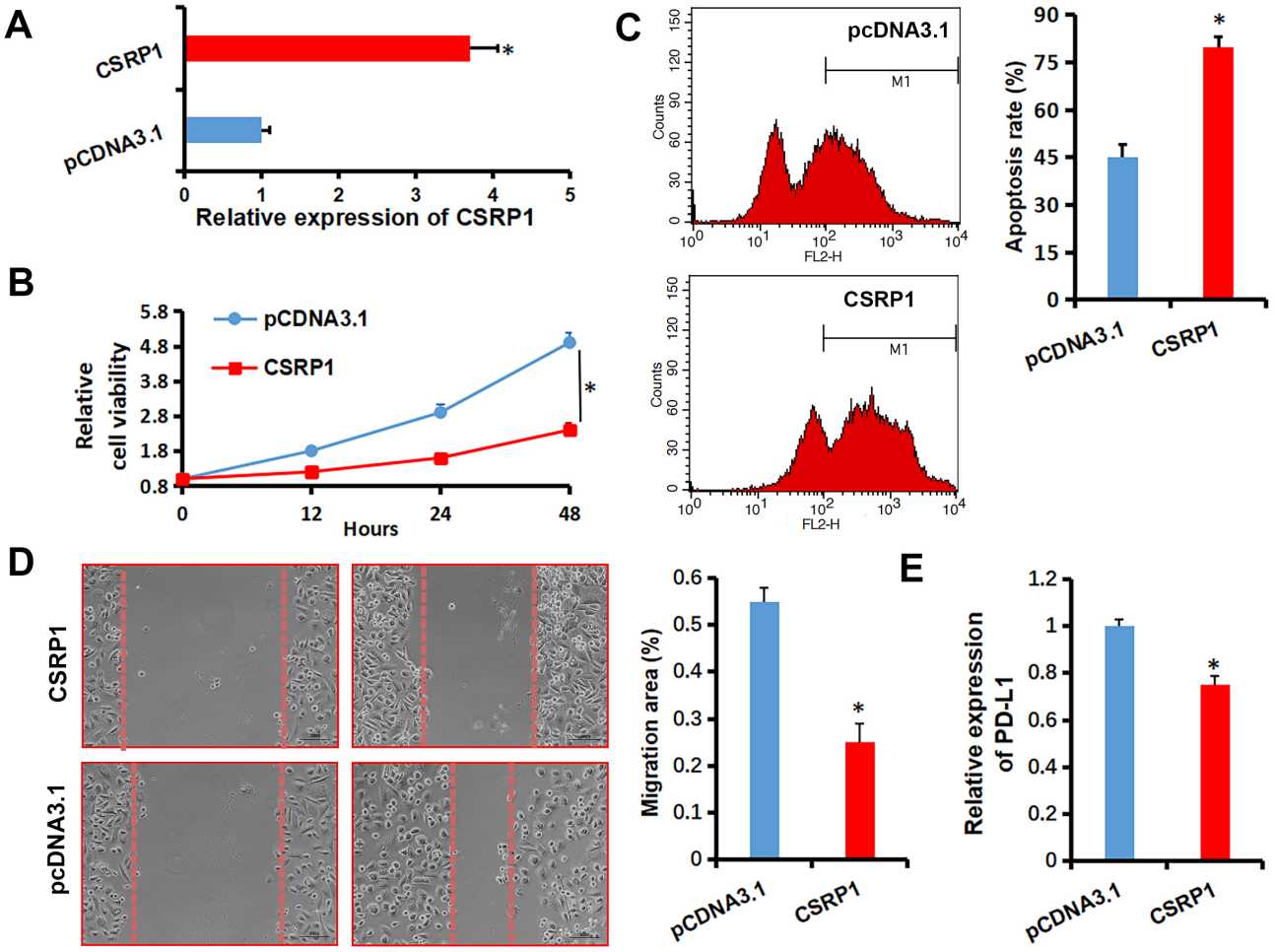

Fig. 1. Effects of *CSRP1* overexpression on malignant phenotypes of RCC cells. (A) qRT-PCR analysis confirming stable overexpression of *CSRP1* in A498 cells transfected with pcDNA3.1-*CSRP1*. (B) Cell viability assessed by CCK-8 assay in *CSRP1*-overexpressing A498 cells. (C) Apoptosis analysis by flow cytometry in A498 cells treated with 10 μM sunitinib. (D) Migratory capacity evaluated by wound healing assay in *CSRP1*-overexpressing A498 cells (Scale bar: 50 μm). (E) qRT-PCR examination for *PD-L1* expression in A498 cells. All data are presented as mean ± SD from three independent experiments (*$p < 0.05$).

were subcutaneously injected into the right flank of each mouse. Twelve days after inoculation, treatment was initiated with intraperitoneal injections of either isotype control (#BE0090) or anti-mouse *PD-L1* antibody (#BE0101, Bio X Cell, West Lebanon, NH, USA) administered at 200 μg per mouse every three days. Tumor dimensions were measured daily using calipers, and volumes were calculated using the formula: volume = length × width^2 / 2. Mice were humanely euthanized with carbon dioxide upon reaching predefined endpoints, including tumor length exceeding 17 mm, weight loss greater than 20%, or the presence of tumor ulceration. Following anesthesia with isoflurane (5% in O_2), tumor development was assessed using a Super Nova® positron emission tomography/computed tomography (PET/CT) system (SNPC-103, Pingsheng Medical Technology, Kunshan, Jiangsu, China), then mice were humanely euthanized with carbon dioxide. Mice were euthanized by gradual displacement of chamber air with compressed carbon dioxide at a flow rate of 30-70% of the chamber volume per minute.

2.7 Statistical Analysis

All statistical analyses were performed using SPSS version 24.0 (SPSS Inc., Armonk, NY, USA). The normality of data distribution was assessed using the Shapiro-Wilk test. Group differences were assessed using one-way analysis of variance (ANOVA). Survival data were analyzed by Kaplan–Meier method, and differences between groups were compared using the log-rank test. A *p*-value of less than 0.05 was considered statistically significant.

3. Results

3.1 CSRP1 Suppressed the RCC A498 Cells Viability and Sensitizes RCC Cells to Sunitinib

To investigate the biological role of *CSRP1* in RCC, we established CSRP1-overexpressing A498 cells (A498-

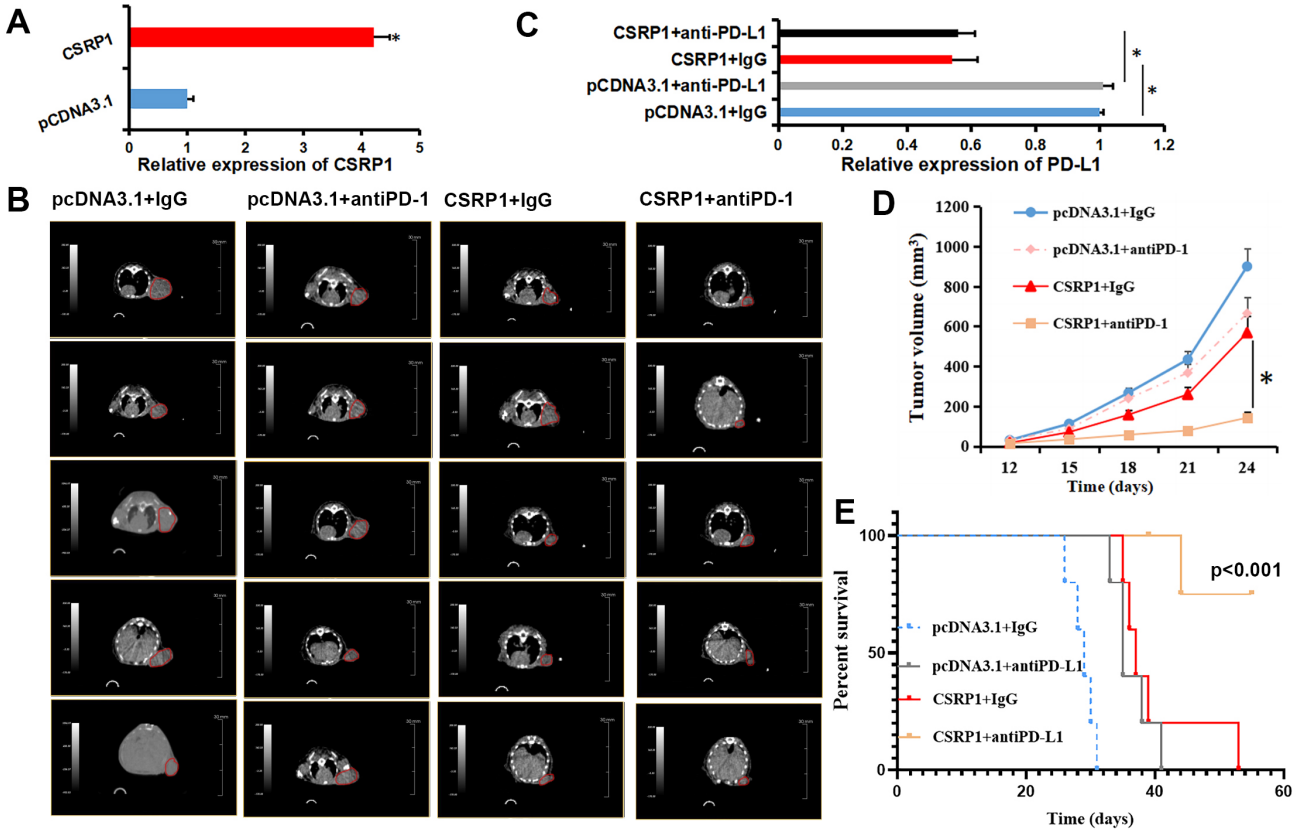

Fig. 2. *CSRP1* overexpression inhibits tumor growth and enhances anti-*PD-L1* therapy response in a murine RCC model. (A) qRT-PCR validation of stable *CSRP1* overexpression in Renca cells. (B) Representative CT images of tumors in the four treatment groups (n = 5). The red circles denote the subcutaneous tumors that were monitored for the study. (C) qRT-PCR examination for *PD-L1* expression in the four treatment groups. (D) Tumor growth curves across experimental groups. (E) Kaplan–Meier survival analysis based on endpoint-free survival (log-rank test, $p < 0.001$). Data are presented as mean ± SD of three independent experiments (*$p < 0.05$).

CSRP1; Fig. 1A). Elevated CSRP1 expression significantly suppressed the viability of A498 cells (Fig. 1B). Apoptosis analysis further revealed that *CSRP1* overexpression markedly increased the sensitivity of A498 cells to sunitinib (10 μM) treatment (Fig. 1C). Additionally, *CSRP1* upregulation considerably attenuated the migratory capacity of A498 cells (Fig. 1D). Given the critical role of *PD-L1* in immunotherapy, we assessed its expression and found that *CSRP1* overexpression significantly reduced *PD-L1* mRNA levels in A498 cells (Fig. 1E). Collectively, these findings suggest that *CSRP1* may function as a tumor suppressor in RCC.

3.2 Overexpression of CSRP1 Decreased Tumor Growth and Enhanced Efficacy of Immunotherapy In Vivo

To further evaluate the impact of *CSRP1* on tumor growth and response to immunotherapy, we employed Renca cells, a murine renal carcinoma cell line, with stable *CSRP1* overexpression (Fig. 2A). Mice were divided into four treatment groups: pcDNA3.1 + IgG, pcDNA3.1 + anti-*PD-L1*, *CSRP1* + IgG, and *CSRP1* + anti-PD-L1 (Fig. 2B). Consistent with the *in vitro* findings, qRT-PCR analysis of the harvested tumor tissues revealed a significant decrease in *PD-L1* mRNA levels in the *CSRP1*-overexpressing groups (Fig. 2C). Results revealed that *CSRP1* overexpression significantly suppressed tumor growth and potentiated the anti-tumor effect of anti-*PD-L1* treatment *in vivo*. Specifically, the *CSRP1* + IgG group exhibited a markedly slower tumor growth rate compared to the pcDNA3.1 + IgG group. Similarly, tumor growth in the pcDNA3.1 + anti-*PD-L1* group was reduced relative to the pcDNA3.1 + IgG controls. Most notably, the combination of *CSRP1* overexpression and anti-*PD-L1* treatment (*CSRP1* + anti-*PD-L1*) led to the strongest inhibition of tumor growth (Fig. 2D). Consistent with these findings, Kaplan–Meier survival analysis indicated a significant prolongation of survival in mice overexpressing *CSRP1* (Fig. 2E). 4 of 5 mice in the *CSRP1* + anti-*PD-L1* group survived until the end of the study, whereas all animals in the other groups reached the predefined survival endpoints. Together, these results demonstrate that *CSRP1* not only inhibits tumor formation and growth in RCC but also enhances the efficacy of anti-*PD-L1* immunotherapy.

4. Discussion

The present study underscores the tumor-suppressive function of *CSRP1* in RCC. Cysteine-rich proteins (*CRP*s), a key subclass within the LIM domain protein family, play vital roles in diverse physiological and pathological contexts. Among them, *CSRP1* has emerged as a potential prognostic biomarker in multiple cancers. Reduced expression of *CSRP1* has been linked to dysregulated cell growth and differentiation, thereby facilitating tumorigenesis [12]. For instance, Demirkol Canli [13] reported that *CSRP1* expression correlates with a mesenchymal stroma-rich molecular subtype and poor prognosis in colon cancer. Similarly, several studies have implicated *CSRP1* in the progression of acute myeloid leukemia (AML). Han *et al*. [14] demonstrated that *METTL3* stabilizes *CSRP1* mRNA through m^6A modification, thereby delaying its degradation. Qin *et al*. [15] associated high *CSRP1* expression with activation of pathways such as *p53*, complement, inflammatory response, *NOTCH*, *IL6-JAK-STAT3*, and *IL2-STAT5* signaling, suggesting its involvement in AML pathogenesis.

Conversely, Lin *et al*. [16] reported that *CSRP1* enhances cisplatin-induced apoptosis and chemosensitivity via mitochondrial pathways in neuroblastoma. In gastric cancer, *CSRP1* was identified as a potential target of Celecoxib [17]. Our previous work revealed that low *CSRP1* expression promotes the progression of hormone-sensitive prostate cancer, a finding supported by clinical cohort analysis [18]. *CSRP1* has also been identified among an eight-gene signature predictive of overall survival in kidney renal papillary cell carcinoma [11]. However, most existing evidence remains bioinformatic, with limited functional validation. To address this gap, we performed systematic *in vitro* functional assays—including proliferation, apoptosis, and migration experiments—which collectively demonstrated that elevated *CSRP1* expression suppresses proliferation, promotes apoptosis, and impedes migration in RCC cells.

Notably, multiple studies have associated high *CSRP1* expression with increased immune infiltration, suggesting a role in modulating antitumor immunity. For example, Wang *et al*. [19] revealed that astrocytic *PD-L1/PD-1* signaling regulates maturation and morphogenesis via the *MEK/ERK* pathway through CSRP1. Qin *et al*. [15], using the GeneMANIA database, identified *ILK*, *MYL9*, *MYLK*, and *REL* as key *CSRP1*-interacting proteins. Based on literature review, we hypothesize that CSRP1 may participate in inflammatory regulation. For instance, ILK upregulation promotes ICAM-1 and *VCAM*-1 expression, potentially amplifying inflammatory responses [20]. *MYL9* facilitates the recruitment of activated T cells to inflamed or tumor tissues [21], while *MYLK* is implicated in immune and inflammatory pathways [22]. *REL* can activate *NOTCH* signaling via Jagged1, influencing B-cell function [23]. To corroborate these findings under more physiologically relevant conditions, we employed syngeneic mouse models, which confirmed that *CSRP1* overexpression restrains tumor growth and synergizes with anti-*PD-L1* therapy. Crucially, our study provides a plausible mechanism for this synergy: the downregulation of *PD-L1* by *CSRP1*. We demonstrated that *CSRP1* overexpression reduces *PD-L1* levels in both cultured RCC cells and murine tumor tissues. This reduction in the primary ligand for *PD-1* likely leads to a diminished *PD-1/PD-L1*-mediated immunosuppressive signal, thereby "priming" the tumor microenvironment for a more effective response when the pathway is therapeutically blocked by anti-*PD-L1* antibodies.

The clinical gain anticipated from our findings is twofold. First, *CSRP1* expression could serve as a novel predictive biomarker to stratify RCC patients for therapy. Our data indicate that tumors with high *CSRP1* levels are not only inherently less aggressive but also more susceptible to anti-*PD-L1* immunotherapy. This suggests that assessing *CSRP1* status in patient tumors could help identify individuals most likely to derive significant benefit from immune checkpoint inhibitors, thereby personalizing treatment approaches and avoiding ineffective therapies in non-responders. Second, and more prospectively, our work nominates *CSRP1* as a compelling therapeutic target itself. The development of strategies to reactivate or mimic *CSRP1* function could represent a new avenue for RCC treatment. Such an approach would aim to restore this natural tumor-suppressive mechanism, simultaneously impairing cancer cell viability and sensitizing the tumor microenvironment to immunotherapy, creating a synergistic antitumor effect.

Despite these significant observations, our study has limitations. Although we demonstrated that *CSRP1* overexpression reduces cell viability and enhances immunotherapy response, the precise molecular mechanisms remain unexplored. Further investigations are warranted to elucidate the signaling pathways and immune-modulatory mechanisms through which *CSRP1* exerts its antitumor effects in RCC.

5. Conclusion

CSRP1 may play a critical role in regulating cell viability, migration, drug resistance, and innate immune responses in RCC. Targeting *CSRP1* could therefore represent a promising therapeutic strategy for RCC treatment. However, further high-quality clinical evidence is needed to validate its translational potential.

Availability of Data and Materials

The data analyzed during the current study are available from the corresponding author on reasonable request.

Author Contributions

YH: Methodology, Software, Data Curation, Writing—Original Draft. Supervision, Validation. YK: Methodology, Data Curation, Writing—Original Draft. Supervision, Validation. DZ: Methodology, Writing—Original Draft, Supervision, Validation. YY: Writing—Review & Editing, Supervision, Validation. BY: Methodology, Software, Data Curation, Writing—Review & Editing, Supervision, Project administration. All authors read and approved the final manuscript. All authors have participated sufficiently in the work and agreed to be accountable for all aspects of the work.

Ethics Approval and Consent to Participate

The animal experiments in this study were conducted in strict compliance with the ARRIVE guidelines, the UK. Animals (Scientific Procedures) Act 1986 and its associated guidelines, and the EU Directive 2010/63/EU. All procedures were reviewed and approved by the Animal Ethics Committee of Dalian Medical University (Permit Number: AEE24139).

Acknowledgment

Not applicable.

Funding

This study was supported by the "1+X" Research Project of the Second Hospital of Dalian Medical University (CYQH2024016) to YH; the Dalian Medical Science Research Program Project (2312015) to YH; Dalian Municipal Guidance Plan Initiative for the Life and Health Sector (2024ZDJH01PT113) to YH; Liaoning Provincial Department of Education Key Research Project (JYTZD2023020) to DZ; Liaoning Provincial Department of Education Basic Scientific Research Project (LJ212510161015) to BY.

Conflict of Interest

The authors declare no conflict of interest.

References

[1] Nierengarten MB. Global cancer statistics 2022: The report offers a view on disparities in the incidence and mortality of cancer by sex and region worldwide and on the areas needing attention. Cancer. 2024; 130: 2568. https://doi.org/10.1002/cncr.35444.

[2] Cheng S, Lin Q, Chen K, Wang J, Peng H, Huang Y, *et al*. NME4: A novel metabolic-associated biomarker for prognosis prediction and immunotherapy response evaluation in clear cell renal cell carcinoma. Molecular Immunology. 2025; 184: 149–163. https://doi.org/10.1016/j.molimm.2025.06.011.

[3] Wang H, Chen Y, Yang Y, Song R, Gu S, Cao X, *et al*. MAGI3 enhances sensitivity to sunitinib in renal cell carcinoma by suppressing the MAS/ERK axis and serves as a prognostic marker. Cell Death & Disease. 2025; 16: 102. https://doi.org/10.1038/s41419-025-07427-0.

[4] Kadrmas JL, Beckerle MC. The LIM domain: from the cytoskeleton to the nucleus. Nature Reviews. Molecular Cell Biology. 2004; 5: 920–931. https://doi.org/10.1038/nrm1499.

[5] Sadler I, Crawford AW, Michelsen JW, Beckerle MC. Zyxin and cCRP: two interactive LIM domain proteins associated with the cytoskeleton. The Journal of Cell Biology. 1992; 119: 1573–1587. https://doi.org/10.1083/jcb.119.6.1573.

[6] Weiskirchen R, Bister K. Suppression in transformed avian fibroblasts of a gene (crp) encoding a cysteine-rich protein containing LIM domains. Oncogene. 1993; 8: 2317–2324.

[7] Xu F, Zhang P, Yuan M, Yang X, Chong T. Bioinformatic screening and identification of downregulated hub genes in adrenocortical carcinoma. Experimental and Therapeutic Medicine. 2020; 20: 2730–2742. https://doi.org/10.3892/etm.2020.8987.

[8] Chen X, Ma J, Xu C, Wang L, Yao Y, Wang X, *et al*. Identification of hub genes predicting the development of prostate cancer from benign prostate hyperplasia and analyzing their clinical value in prostate cancer by bioinformatic analysis. Discover Oncology. 2022; 13: 54. https://doi.org/10.1007/s12672-022-00508-y.

[9] Fujita A, Gomes LR, Sato JR, Yamaguchi R, Thomaz CE, Sogayar MC, *et al*. Multivariate gene expression analysis reveals functional connectivity changes between normal/tumoral prostates. BMC Systems Biology. 2008; 2: 106. https://doi.org/10.1186/1752-0509-2-106.

[10] Wang L, Liu X, Yue M, Liu Z, Zhang Y, Ma Y, *et al*. Identification of hub genes in bladder cancer based on weighted gene co-expression network analysis from TCGA database. Cancer Reports. 2022; 5: e1557. https://doi.org/10.1002/cnr2.1557.

[11] Luo Y, Chen D, Xing XL. Comprehensive Analyses Revealed Eight Immune Related Signatures Correlated With Aberrant Methylations as Prognosis and Diagnosis Biomarkers for Kidney Renal Papillary Cell Carcinoma. Clinical Genitourinary Cancer. 2023; 21: 537–545. https://doi.org/10.1016/j.clgc.2023.06.011.

[12] Zhou CZ, Qiu GQ, Wang XL, Fan JW, Tang HM, Sun YH, *et al*. Screening of tumor suppressor genes on 1q31.1-32.1 in Chinese patients with sporadic colorectal cancer. Chinese Medical Journal. 2008; 121: 2479–2486.

[13] Demirkol Canli S. CSRP1 expression is associated with a mesenchymal, stroma-rich tumor profile and poor prognosis in colon cancer. Turkish Journal of Medical Sciences. 2023; 53: 1678–1689. https://doi.org/10.55730/1300-0144.5736.

[14] Han L, Wang R, He M, Chen Z, Wang F. METTL3/YTDHF1 Stabilizes CSRP1 mRNA to Regulate Glycolysis and Promote Acute Myeloid Leukemia Progression. Cell Biochemistry and Biophysics. 2025; 83: 1993–2007. https://doi.org/10.1007/s12013-024-01610-4.

[15] Qin L, Li B, Wang S, Tang Y, Fahira A, Kou Y, *et al*. Construction of an immune-related prognostic signature and lncRNA-miRNA-mRNA ceRNA network in acute myeloid leukemia. Journal of Leukocyte Biology. 2024; 116: 146–165. https://doi.org/10.1093/jleuko/qiae041.

[16] Lin YH, Jiang JH, Chuang HC, Huang CC, Hsu WM, Wu MT, *et al*. The Involvement of CSRP1 in Neuroblastoma Differentiation and Apoptosis Impacting Tumor-Suppressive Therapeutic Responses. FASEB Journal. 2025; 39: e70521. https://doi.org/10.1096/fj.202500403R.

[17] Jin GH, Xu W, Shi Y, Wang LB. Celecoxib exhibits an antigastric cancer effect by targeting focal adhesion and leukocyte transendothelial migration-associated genes. Oncology Letters. 2016; 12: 2345–2350. https://doi.org/10.3892/ol.2016.4976.

[18] Pan C, Wang W, He Y, Yang B. Identification of CSRP1 as novel biomarker for hormone-sensitive prostate cancer by the combination of clinical and functional research. Cancer Cell International. 2025; 25: 65. https://doi.org/10.1186/s12935-025-03708-y.

[19] Wang Y, Zhang M, Zhang T, Zhang S, Ji F, Qin J, *et al*.

PD-L1/PD-1 checkpoint pathway regulates astrocyte morphogenesis and myelination during brain development. Molecular Psychiatry. 2025; 30: 3895–3911. https://doi.org/10.1038/s41380-025-02969-3.

[20] Hortelano S, López-Fontal R, Través PG, Villa N, Grashoff C, Boscá L, *et al*. ILK mediates LPS-induced vascular adhesion receptor expression and subsequent leucocyte trans-endothelial migration. Cardiovascular Research. 2010; 86: 283–292. https://doi.org/10.1093/cvr/cvq050.

[21] Lv M, Luo L, Chen X. The landscape of prognostic and immunological role of myosin light chain 9 (MYL9) in human tumors. Immunity, Inflammation and Disease. 2022; 10: 241–254. https://doi.org/10.1002/iid3.557.

[22] Liu T, Zhuang XX, Qin XJ, Wei LB, Gao JR. Alteration of N6-methyladenosine epitranscriptome profile in lipopolysaccharide-induced mouse mesangial cells. Naunyn-Schmiedeberg's Archives of Pharmacology. 2022; 395: 445–458. https://doi.org/10.1007/s00210-022-02208-4.

[23] Bash J, Zong WX, Banga S, Rivera A, Ballard DW, Ron Y, *et al*. Rel/NF-kappaB can trigger the Notch signaling pathway by inducing the expression of Jagged1, a ligand for Notch receptors. The EMBO Journal. 1999; 18: 2803–2811. https://doi.org/10.1093/emboj/18.10.2803.